

Latent Poincaré Shaping for Agentic Reinforcement Learning

Hanchen Xia[†], Baoyou Chen[†], Zelin Zang^{*}, Yutang Ge[‡],
 Guojiang Zhao[§], Siyu Zhu^{†◊1}

[†]Shanghai Academy of AI for Science,

^{*}Centre for Artificial Intelligence and Robotics, HKISI-CAS

[‡]School of Mathematical Sciences, Shanghai Jiao Tong University,

[§]Carnegie Mellon University, [◊]Fudan University

xiahanchen2000@icloud.com

Abstract

We propose LAPHA, a method for training AlphaZero-like LLM agents in a Poincaré latent space. Under LAPHA, the search process can be visualized as a tree rooted at the prompt and growing outward from the origin toward the boundary of the Poincaré ball, where negative curvature provides exponentially increasing capacity with radius. Using hyperbolic geodesic distance to rule-verified correctness, we define a node potential and assign dense process rewards by potential differences. We further attach a lightweight value head on the same shared latent space, enabling self-guided test-time scaling with almost no additional overhead. On MATH-500, LAPHA improves Qwen2.5-Math-1.5B from 66.0% to 88.2%. With value-head-guided search, LAPHA-1.5B reaches 56.7% accuracy on AIME’24, and LAPHA-7B further achieves 60.0% on AIME’24 and 53.3% on AIME’25.

1. Introduction

Large language models (LLMs) can solve challenging problems, but their default behavior is still single-pass generation: producing an entire solution in one trajectory. For tasks that require multi-step reasoning, tool use, and self-correction, a common remedy is to scale test-time compute by explicitly searching over action-observation traces and selecting better outcomes from multiple candidates (Yao et al., 2022; 2023). In this view, a dialogue prefix (including tool feedback) defines

a state, each next-step completion defines an action, and repeated branching induces a behavior tree.

Monte Carlo Tree Search (MCTS) provides a principled way to explore such trees, and has historically paired well with a policy prior and a learned value function for strong planning (Silver et al., 2017). However, the “game of natural language” differs from board games in a key respect: the action space is not a small, fixed set. An action is a variable-length token sequence, and the branching factor is dominated by semantic aliasing—many distinct strings correspond to near-identical meaning (paraphrases, formatting variants, and tool-call surface forms) (Wang et al., 2022; Farquhar et al., 2024). Meanwhile, in RL with verifiable rewards (RLVR), rule-based checkers label only a tiny fraction of leaves as correct (Zhang et al., 2025; Wang et al., 2025). Together, aliasing and sparse terminal signals make token-space exploration wasteful and credit assignment brittle.

This paper takes the position that token sequences are an inconvenient interface for search and learning, while backbone hidden states provide a more faithful representation of “state” and “policy”. Ideally, we want a latent semantic space equipped with a distance such that progress along a reasoning trace can be measured geometrically. If such a distance is available, it enables three capabilities: (i) converting sparse terminal verification into dense process rewards by shaping intermediate nodes via distance-to-goal; (ii) training a lightweight value estimator on the same latent states to guide MCTS without relying on heavyweight reward-/value models at inference; and (iii) pruning redundant branches by clustering in latent space rather than by brittle string matching.

¹Corresponding author.

The obstacle is geometry. Modern decoder backbones with normalization such as RMSNorm tend to produce representations with near-constant activation scale (Zhang & Sennrich, 2019; Yang et al., 2025), making Euclidean norms and Euclidean distances poor proxies for semantic progress. More broadly, bounded or nonnegative-curvature geometries (including spherical representations) force deep trees to be packed into limited effective capacity, increasing crowding and eroding distance contrast across depths—exactly the failure mode that undermines distance-based progress signals.

A classical remedy is negative curvature. Hyperbolic spaces expand exponentially with radius, matching the combinatorics of trees, and the Poincaré ball provides a practical model where points stay inside a unit ball while intrinsic (geodesic) distances remain unbounded (Poincaré, 1882; Beardon, 2012). Poincaré embeddings exploit this property to represent hierarchies with low distortion (Nickel & Kiela, 2017; Ganea et al., 2018). We transfer the same geometric insight from word hierarchies to LLM behavior trees by mapping pooled backbone hidden states into a root-centered Poincaré latent space.

We propose LAPHA (Poincaré **Latent AlPhaZero-like** RL for **agentic** reasoning), an AlphaZero-like agentic reinforcement learning framework in which a single shared, root-centered Poincaré latent space serves as the interface between search and learning (Fig. 1c). All components operate on this shared representation:

- (i) **Geodesic potential shaping** converts sparse terminal verification into dense process rewards over the rollout tree;
- (ii) **A lightweight value head** trained on the same pooled hidden state learns a correctness-aligned ranking signal, enabling self-guided Monte Carlo Tree Search for test-time scaling with minimal overhead;
- (iii) **Latent-space pruning** clusters and removes paraphrastic near-duplicates to preserve diversity and reduce wasted expansions.

Across our math-reasoning experiments, LAPHA yields consistent improvements; with self-guided search, LAPHA on Qwen2.5-Math-7B achieves 60.0% on AIME’24 and 53.3% on AIME’25, outperforming `o1-mini` on these benchmarks.

2. Methodology

2.1. Root-centered latent states in the Poincaré ball

In MCTS, the decision rule at a node can be written as a policy $\pi_\theta(a | s)$. For an LLM-based agent, the state s at node i is the serialized dialogue prefix produced by `apply_chat_template` (including the system/user messages, previous assistant steps, and any tool feedback), while the action a is the next-step completion generated by the model (including an explicit end-of-turn token, in our case `<|im_end|>`). Concatenating the state and action yields a single context sequence of length L , and a forward pass through the decoder produces the final-layer hidden states $\mathbf{h}_{1:L}^{(i)} \in \mathbb{R}^{L \times H}$. As illustrated in Fig. 1(a), compact geometries with bounded intrinsic scale can crowd deep states and reduce long-range contrast, motivating a hyperbolic latent construction for tree-structured reasoning. We summarize this token-level representation into a single vector by mean pooling:

$$\bar{\mathbf{h}}_i = \frac{\sum_{t=1}^L m_{i,t} \mathbf{h}_t^{(i)}}{\sum_{t=1}^L m_{i,t}}, \quad m_{i,t} = \mathbb{I}_{[t \neq <|endoftext|>]} \quad (1)$$

where `<|endoftext|>` is used as the padding token in our implementation (In practice, we input a batch of contexts with different lengths, so we pad sequences to a common length). Let $\hat{\mathbf{h}}_0$ denote the pooled vector at the root. For any node i , we translate the hidden state by $\bar{\mathbf{h}}_i - \hat{\mathbf{h}}_0$ and then map it into the Poincaré ball:

$$\mathbf{y}_i = \exp_0 \left(\frac{\bar{\mathbf{h}}_i - \hat{\mathbf{h}}_0}{\sqrt{H}} \right) \in \mathbb{D}^H, \quad \mathbb{D}^H = \{\mathbf{y} \in \mathbb{R}^H : \|\mathbf{y}\|_2 < 1\}. \quad (2)$$

The exponential map at the origin is defined as

$$\exp_0(\mathbf{v}) = \tanh(\|\mathbf{v}\|_2) \frac{\mathbf{v}}{\|\mathbf{v}\|_2 + \delta}, \quad (3)$$

where δ is a small constant for numerical stability (and we additionally apply a tiny projection margin in finite precision to ensure $\|\mathbf{y}_i\|_2 < 1$). Since $\mathbf{y}_0 = \exp_0(\mathbf{0}) = \mathbf{0}$, the agent’s reasoning tree in the Poincaré ball grows outward from the origin toward the boundary. Here the root node corresponds exactly to the original prompt p_0 .

2.2. Poincaré potential shaping

We first define the hyperbolic geodesic distance on the Poincaré ball (curvature fixed to 1 in our implementation). For any $\mathbf{u}, \mathbf{v} \in \mathbb{D}^H$,

$$d_{\mathbb{D}}(\mathbf{u}, \mathbf{v}) = \text{arcosh} \left(1 + 2 \frac{\|\mathbf{u} - \mathbf{v}\|_2^2}{(1 - \|\mathbf{u}\|_2^2)(1 - \|\mathbf{v}\|_2^2)} \right). \quad (4)$$

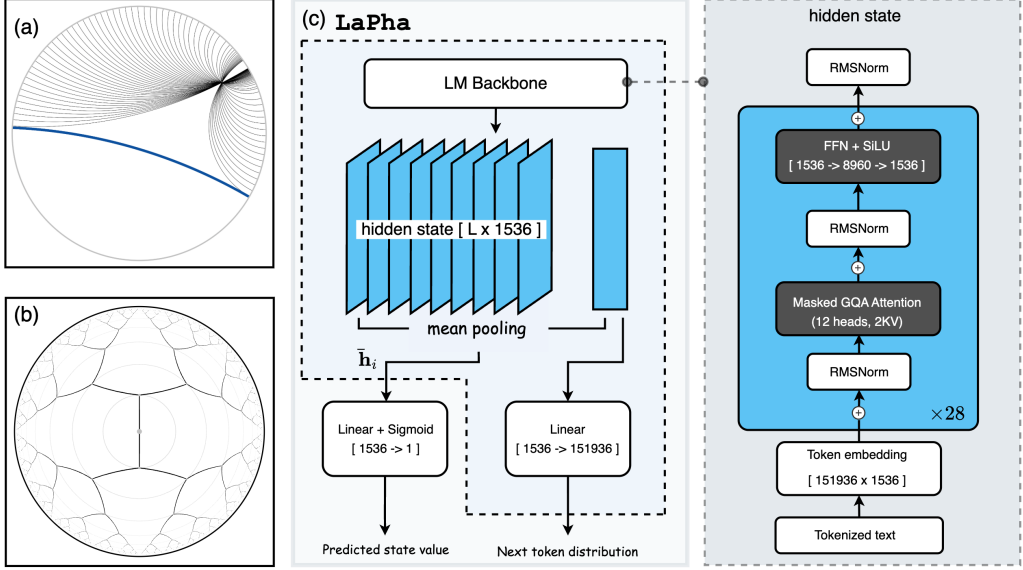


Figure 1. Overview of LAPHA. (a) In the Poincaré disk model of hyperbolic geometry, straight lines are geodesics—Euclidean circular arcs orthogonal to the unit circle (or diameters); the figure illustrates a family of hyperbolic parallel lines that share an ideal boundary point. (b) A hyperbolic tiling in the Poincaré disk, visualizing the rapid expansion of effective capacity with radius in negative curvature. (c) LAPHA mean-pools the backbone hidden states to obtain a node representation, maps it into a prompt-centered Poincaré latent state, and reuses this shared latent space for geodesic potential shaping, value estimation, and latent-space pruning in search.

$d_{\mathbb{D}}(\mathbf{u}, \mathbf{v})$ inherits the exponential expansion of effective capacity with radius, which is well matched to the branching structure of reasoning trees (Fig. 1(b)). After an MCTS rollout, each node i is associated with a latent point $\mathbf{y}_i \in \mathbb{D}^H$. In RLVR, terminal nodes can be verified by a rule-based checker (e.g., whether an extracted answer matches the ground truth); we denote the hidden states of verified-correct terminal leaves by \mathcal{Y}^+ . Since we construct latents in a root-centered manner, the root node satisfies $\mathbf{y}_0 = \mathbf{0}$.

For any node i , we define its distance to the closest successful leaf and its distance to the root as

$$d_i^{[\text{goal}]} = \min_{\mathbf{y}_\omega \in \mathcal{Y}^+} d_{\mathbb{D}}(\mathbf{y}_i, \mathbf{y}_\omega), \quad d_i^{[\text{root}]} = d_{\mathbb{D}}(\mathbf{y}_i, \mathbf{0}). \quad (5)$$

We then construct a bounded geodesic potential

By construction, $V(0) \approx 0$, and for any $\mathbf{y}_\omega \in \mathcal{Y}^+$ we have $V(\omega) = 1$. This is a standard potential-based shaping design: shaping with potential differences preserves the optimal policy of the underlying MDP (Ng et al., 1999; Wiewiora, 2003; Devlin & Kudenko, 2012). Given an edge $(i \rightarrow j)$ on a sampled reaction chain, we convert the potential into a step reward

$$r(i, j) = V(j) - V(i). \quad (7)$$

2.3. AlphaZero-like Monte Carlo Tree Search

We attach a lightweight value head to the same pooled backbone representation $\bar{\mathbf{h}}(s)$ used to define the latent state (Fig. 1(c)). Concretely, the value head is a linear predictor with sigmoid,

$$f_\phi(\bar{\mathbf{h}}(s)) = \sigma(\mathbf{w}^\top \bar{\mathbf{h}}(s) + b) \in (0, 1), \quad (8)$$

and we supervise it using the Poincaré potential target $V(s)$ with an MSE loss,

$$\mathcal{L}_{\text{value}} = \mathbb{E} \left[(f_\phi(\bar{\mathbf{h}}(s)) - V(s))^2 \right]. \quad (9)$$

After training, f_ϕ serves as a learned heuristic during search, while terminal nodes are still assigned verifiable outcomes by rule-based reward functions.

During rollout, we run MCTS where (i) candidate priors are induced by the model’s cumulative log-probabilities and (ii) unvisited edges are initialized by a convex combination of the value-head prediction and this likelihood prior; only verified terminal outcomes are backed up as returns. The complete specification (search space, statistics, selection/expansion/evaluation/backup) is given in Appendix A.1.

Latent-space pruning. Language actions admit heavy paraphrastic aliasing, which can waste search budget

on near-duplicate branches. We periodically prune the search frontier in the same root-centered Poincaré latent space: we cluster visited non-terminal nodes by hyperbolic distance and disable a fraction of nodes within each cluster, then rebuild the frontier and continue search. This pruning step improves action-space coverage under a fixed rollout budget and is summarized in Appendix A.1 (Algorithm 1 and Algorithm 2).

2.4. Policy Optimization

After batch rollout, we obtain search trees where terminal leaves are labeled as success/failure by rule-based verification. To avoid degenerate learning signals (e.g., almost-always-correct or almost-always-wrong rollouts), we filter rollout trees by their empirical success rate and keep only those within $(0.0, 0.8]$. From the retained trees we sample n groups for each policy update. Each group corresponds to one prompt q and a set of G sampled continuations $\{o_i\}_{i=1}^G$.

For each continuation o_i , we compute a scalar return $R(q, o_i)$ by aggregating the dense step rewards along its root-to-leaf path (and optionally adding lightweight format bonuses). We then optimize the policy using Dr. GRPO (Liu et al., 2025). Define the token-wise likelihood ratio

$$r_{i,t} = \frac{\pi_\theta(o_{i,t} | q, o_{i,<t})}{\pi_{\theta_{\text{old}}}(o_{i,t} | q, o_{i,<t})}, \quad (10)$$

and the centered group advantage (shared across tokens of the same continuation)

$$\hat{A}_i = R(q, o_i) - \frac{1}{G} \sum_{k=1}^G R(q, o_k). \quad (11)$$

The clipped objective for one group is

$$\mathcal{L}_{\text{policy}} = -\frac{1}{G} \sum_{i=1}^G \sum_{t=1}^{|o_i|} \min(r_{i,t} \hat{A}_i, \text{clip}(r_{i,t}, 1 - \epsilon, 1 + \epsilon) \hat{A}_i), \quad (12)$$

and we average $\mathcal{L}_{\text{policy}}$ across the sampled groups in the update batch.

In this work, we additionally keep a small KL regularization coefficient ($\beta = 10^{-8}$) to damp abrupt distribution shifts; its effect is negligible in magnitude and we omit the explicit KL term from the main objective for clarity (Schulman et al., 2017; Shao et al., 2024). Finally, we jointly optimize the policy and value objectives with a fixed weight: $\mathcal{L} = \mathcal{L}_{\text{policy}} + \lambda \mathcal{L}_{\text{value}}$, $\lambda = 0.1$.

3. Experiments

3.1. Basic settings

We start training from the Qwen2.5 family and adopt a two-stage pipeline: supervised cold-start training followed by MCTS-based agentic RL.

We first perform 2 epochs of SFT on a mixture of Glaive v2 training dataset ², OpenR1-Math-220k ³, and a format-adapted version of NuminaMath-TIR (Beeching et al., 2024). The converted NuminaMath-TIR format and the full SFT hyperparameters are provided in Appendix A.3.

After the cold-start, we run 4 epochs of RL. At each update step, we roll out at most 16 prompts; for each problem, we run MCTS to collect one search tree. We filter out degenerate rollouts by keeping only trees whose empirical success rate lies in $(0, 0.8]$, and then construct training groups from the remaining trees. To ensure the shaping signal is non-trivial, we further require that the range of rewards on the tree exceeds 1.0×10^{-2} , and we keep at most 8 such groups per update step (once 8 groups are collected, we terminate the rollout stage early, which may drop a small fraction of samples within an epoch). We set the warmup ratio to 0.05 and the learning rate to 1.0×10^{-6} . Additional training details are deferred to Appendix A.5.

We train LAPHA on DAPO-Math-17K ⁴ (Yu et al., 2025) and evaluate on AIME’24, AIME’25 (aim), Olympiad-Bench (He et al., 2024), MATH-500 (Hendrycks et al., 2021), and Gaokao’23 (En) (Zhang et al., 2023). Unless otherwise stated, all reported numbers are averaged over 16 independent generations at test time. We also run test-time scaling via self-guided MCTS using the attached value head; the search configuration follows the rollout setting unless explicitly noted.

3.2. General Performance of LaPha

Table 1 summarizes the overall performance of LAPHA across a range of base models and math-reasoning benchmarks. Across all evaluated backbones, LAPHA consistently improves over the corresponding base models and strong RL baselines, with gains that further amplify under value-guided self-guidance at test time.

²<https://huggingface.co/datasets/glaiveai/glaive-function-calling-v2>

³<https://huggingface.co/datasets/open-r1/OpenR1-Math-220k>

⁴<https://huggingface.co/datasets/BytedTsinghua-SIA/DAPO-Math-17k>

Base model	Method Train / Test	Tool	Competition and College Level				OOD Gaokao'23 (En)
			AIME'24	AIME'25	Olympiad	MATH	
Qwen2.5-1.5B	—	✗	0.9	0.4	4.1	35.0	19.7
	DAPO	✗	6.7	6.7	22.2	59.0	42.3
	LAPHA	✓	12.7	10.4	20.8	56.6	43.4
	LAPHA / sg@128	✓	20.0 +19.1	16.7 +16.3	24.3 +20.2	64.2 +29.2	50.1 +30.4
Qwen2.5-Math-1.5B	—	✗	3.3	10.0	31.0	66.0	46.5
	—	✓	23.3	13.3	41.3	73.8	53.7
	DAPO	✗	20.0	14.4	42.7	76.0	59.1
	ToRL	✓	26.7	26.7	44.0	77.8	—
	LAPHA	✓	30.0	26.7	38.0	79.6	58.8
Qwen2.5-7B	LAPHA / sg@128	✓	56.7 +53.3	43.3 +30.0	40.0 +9.0	88.2 +22.2	67.7 +21.2
	—	✗	9.1	6.7	21.3	56.9	36.4
	TREEPO / maj@16	✗	28.9	—	49.2	—	—
	DAPO	✗	16.7	16.7	37.9	77.4	63.2
Qwen2.5-Math-7B	LAPHA / sg@128	✓	46.7 +37.6	53.3 +46.7	46.0 +24.7	86.0 +29.1	71.4 +35.0
	—	✗	10.0	16.7	32.4	74.8	37.1
	—	✓	26.7	16.7	45.0	78.8	39.0
	DAPO	✗	36.7	23.3	43.5	83.0	44.0
	SIMPLERL	✗	33.3	6.7	37.6	77.2	—
	PRIME	✗	26.7	13.3	42.1	79.2	—
GPT-4o	ToRL	✓	43.3	30.0	49.9	82.2	—
	LAPHA / sg@128	✓	60.0 +50.0	53.3 +36.7	58.0 +25.6	92.0 +17.2	74.3 +37.2
GPT-o1-mini	-	✗	9.3	5.8	43.3	76.6	67.5
GPT-o1-mini	-	✗	56.7	51.7	65.3	90.0	78.4

Table 1. General performance of LAPHA across base models and math-reasoning benchmarks. We report accuracy (%) on AIME'24, AIME'25, OlympiadBench, MATH-500, and Gaokao'23 (En). SFT denotes our cold-start supervised finetuning baseline under the same data format and evaluation pipeline. LAPHA/sg@128 denotes self-guidance at test time: we run value-guided MCTS with 128 simulations per prompt and select the terminal leaf with the highest predicted state value. Blue cells highlight our runs (and the annotated improvements are relative to the corresponding base model in the same block).

On Qwen2.5-Math-1.5B, LAPHA raises accuracy on AIME'24/AIME'25 from 3.3/10.0 to 30.0/26.7, and self-guided search with 128 MCTS simulations per prompt (sg@128) further boosts performance to 56.7/43.3. On MATH-500, the same model improves from 66.0 to 79.6 under training-time LAPHA, and reaches 88.2 with self-guidance, demonstrating that the learned value signal enables effective test-time scaling without relying on a heavyweight external value model. We also observe consistent gains on the out-of-distribution Gaokao'23 (En) benchmark, indicating improved robustness beyond in-domain math problems. For larger backbones, LAPHA continues to scale favorably. On Qwen2.5-Math-7B, self-guided LAPHA achieves 92.0 accuracy on MATH-500, while reaching 60.0 and 53.3 on AIME'24 and AIME'25, respectively—results that are comparable to or surpass contemporaneous frontier models such as GPT-o1-mini.

Improvements on OlympiadBench are comparatively smaller for 1.5B-scale models. We attribute this partly to a training-data bias: the ground-truth answers in DAPO-Math-17K are restricted to integers, whereas Olympiad problems often admit diverse symbolic solutions (e.g., expressions involving π or radicals). This

mismatch can bias both the learned policy distribution and the verifier-aligned training signal toward integer-like outputs, limiting transfer to more free-form answer spaces. Notably, this effect is substantially mitigated at the 7B scale, where stronger representational capacity appears to alleviate the bias through improved generalization.

3.3. Ablation: Geometry for Dense Process Rewards

We ablate the geometry used for process-reward shaping while keeping the base model, rollout budget, verification protocol, and policy optimization fixed. All variants share the same root-centered latent points $\{\mathbf{y}_i\}$ and the same return aggregation; the only difference is how the per-edge step reward is constructed.

Let \mathcal{L}^+ be the set of verified-correct terminal leaves, and let $\text{PATH}(i, j)$ denote the set of nodes on the unique simple path from node i to node j in the rollout tree (including endpoints). We propagate leaf-level success to intermediate states by

$$\mathcal{P}^+ = \left(\bigcup_{\omega \in \mathcal{L}^+} \text{PATH}(0, \omega) \right) \setminus \{0\}, \quad (13)$$

which contains exactly the non-root nodes that lie on

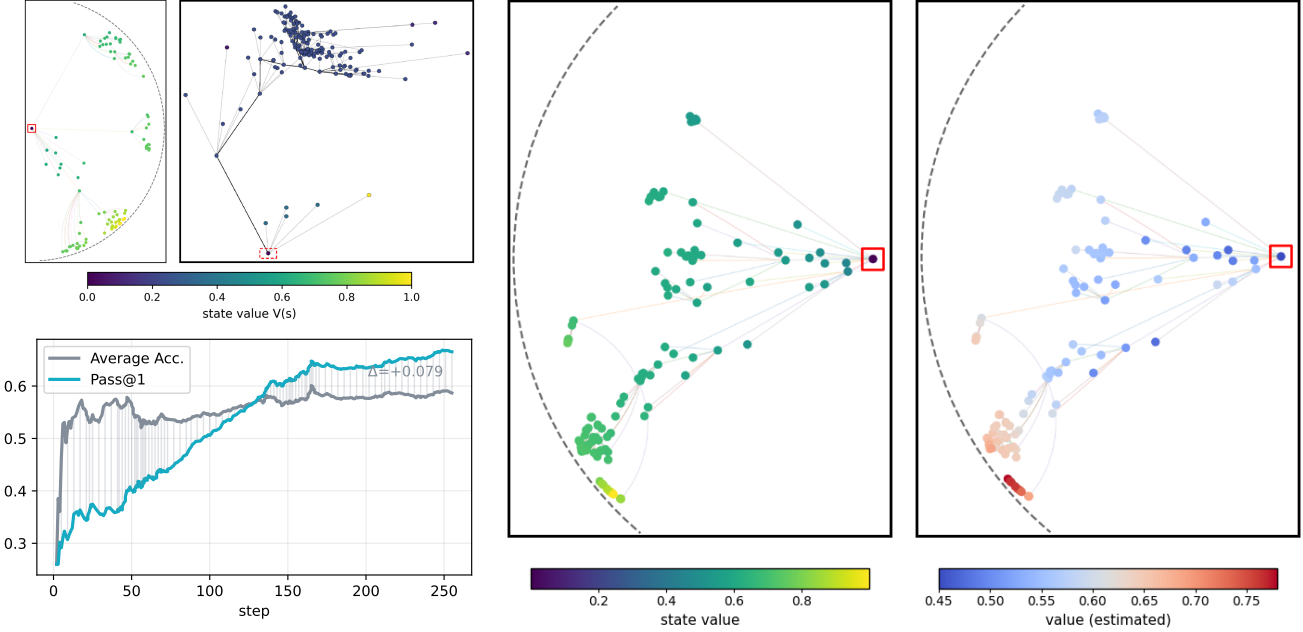


Figure 2. Left-top: Geometry ablation on the same rollout tree: node potentials $V(i)$ computed from the shared root-centered latents using Poincaré geodesic distance (disk view) versus Euclidean distance (ambient-space view). **Left-bottom:** During training, the value head’s top-1 selection (Pass@1) increasingly outperforms the average correctness among terminal leaves (Average Acc.). **Middle:** A guided rollout visualized in the prompt-centered Poincaré disk, colored by the geodesic potential $V(i)$. **Right:** The same rollout colored by the value head prediction $f_\theta(\mathbf{h}_i)$. The red box marks the root (prompt) state.

at least one verified-correct trajectory.

We compare three shaping schemes:

(Sparse). A binary *step reward* that marks whether the next node lies on any verified-correct trajectory,

$$r_{0/1}(i, j) = \mathbb{I}[j \in \mathcal{P}^+]. \quad (14)$$

This baseline provides supervision only on edges belonging to successful trajectories, without introducing any distance-based notion of progress.

(Euclidean). We keep the same potential form $V(i)$ and the same conversion $r(i, j) = V(j) - V(i)$ as in LAPHA, but measure distances in the ambient Euclidean space,

$$d_E(\mathbf{u}, \mathbf{v}) = \|\mathbf{u} - \mathbf{v}\|_2. \quad (15)$$

(Poincaré). The default LAPHA instantiation, where the same potential form and the same potential-to-reward conversion are used, but distances are computed by the Poincaré geodesic metric (defined in the previous subsection).

Discussion. Table 2 shows that hyperbolic shaping consistently outperforms both the binary surrogate (0/1) and Euclidean shaping. Notably, Euclidean shaping is even worse than the coarse 0/1 potential. A

	AIME’24	AIME’25	MATH
Sparse	18.4	16.7	77.4
Euclidean	13.3	10.0	70.5
Poincaré	30.0	26.7	79.6

Table 2. Ablation on the geometry used to define $V(i)$ for process-reward shaping. All settings are identical except the distance metric (or the binary surrogate) used inside $V(i)$.

plausible explanation is that naive Euclidean distances on bounded latent points tend to under-resolve deep states: as search depth increases, many nodes occupy a similar narrow region in the latent space, so d_E yields weak separation and noisy nearest-goal structure. This can inject misleading intermediate rewards, which is arguably why ‘semantic distance’ has often been avoided in practice when the metric is not chosen carefully. In contrast, even the 0/1 surrogate avoids such metric-induced false gradients by providing a coarse but stable signal.

Figure 2 (left-top) provides a geometric intuition. In the Euclidean view (right), deep nodes exhibit stronger crowding and reduced value contrast. In the Poincaré disk (left), points near the boundary may look close un-

der the 2D Euclidean visualization, but the hyperbolic metric expands distances near the boundary, which preserves separation among deep branches; this is reflected by the clearer color stratification in $V_P(i)$ and leads to more informative dense rewards for long-horizon tree learning.

3.4. Journey of the Value Head

We inspect how the value head behaves under latent-space supervision, using Qwen2.5-Math-1.5B and the same rollout/evaluation protocol as in the beginning of this section.

(1) Correctness-aligned ranking beyond likelihood. Figure 2 reports two statistics computed from the same rollout trees. Average Acc. is the mean correctness over all terminal leaves, while Pass@1 evaluates the single terminal leaf selected by the value head (the one with the highest predicted value). The increasing gap indicates that the value head learns to rank competing rollouts by verifiable correctness rather than simply following the policy likelihood ordering. We further ablate whether the value regression loss should update the shared backbone; results are deferred to Appendix A.2.

(2) Value predictions are consistent with the geometry-derived potential. Figure 2 visualizes a guided rollout in the prompt-centered Poincaré disk. For visualization only, we project cached H -dimensional latents to 2D with t-SNE (Maaten & Hinton, 2008). High-value regions under the geodesic potential $V(i)$ largely overlap with regions assigned high predictions by $f_\theta(\bar{\mathbf{h}}_i)$, suggesting that the value head internalizes the same notion of progress used for supervision and can act as a cheap proxy when the success set \mathcal{L}^+ is unknown at test time.

3.5. Test-time scaling

Beyond improving exploration during training, the learned value head also enables test-time scaling without introducing any additional model. We fix the trained LAPHA checkpoint and vary the MCTS simulation budget at inference time. For each prompt, MCTS is guided by the value head during selection, and we return the terminal leaf with the highest predicted state value.

Figure 3 shows a compute–performance trend: allocating more simulations yields better decisions. Notably, the improvement is steep when increasing the budget from 1 to 4–16 simulations, and then gradually saturates, which is consistent with MCTS concentrating

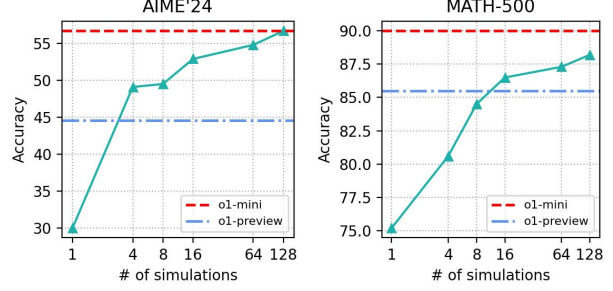


Figure 3. Test-time scaling with value-guided MCTS on AIME'24 and MATH-500. Increasing the number of simulations consistently improves accuracy, with large gains at small budgets and diminishing returns at larger budgets. On AIME'24, accuracy rises from about 30% (1 simulation) to about 56% (128 simulations); on MATH-500 it increases from about 75% to about 88%. Horizontal reference lines are included for comparison.

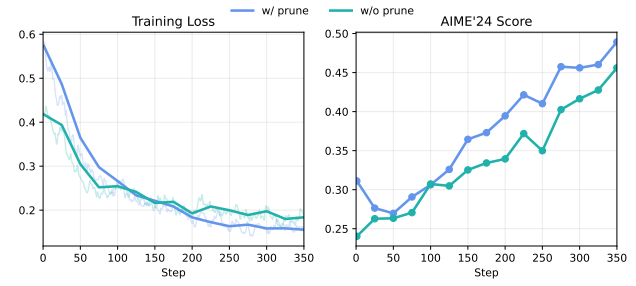


Figure 4. Effect of latent-space pruning. Left: training loss. Right: AIME'24 validation score.

visits on a small set of promising subtrees once a reliable heuristic is available.

3.6. Pruning enables fuller action-space exploration

We keep the overall training and evaluation protocol fixed, and only ablate whether latent-space pruning is enabled. When pruning is enabled, we run MCTS with a fixed simulation budget per prompt and periodically perform global clustering + pruning on visited non-terminal nodes.

Figure 4 shows that pruning improves both optimization and generalization. The pruning run begins with a slightly higher loss, consistent with pruning preventing the search from repeatedly expanding a small set of high-likelihood paraphrases and instead forcing exploration into less-visited regions. After this transient, pruning converges faster and reaches a lower final loss, suggesting that rollout data become less redundant and provide higher-quality learning signals.

The right panel shows a persistent advantage on

AIME’24 validation. We attribute this to reduced semantic collapse of the frontier: without pruning, many expansions concentrate in dense paraphrase clusters, so a large fraction of simulations revisit near-duplicate states. Pruning counteracts this by clustering nodes in the shared latent space and removing a fraction of near-duplicates, reallocating budget to under-explored semantic regions and increasing the chance of discovering rare-but-correct solution paths.

4. Related Work

Verifiable rewards for reasoning and outcome-supervised RL. A growing body of work uses verifiable rewards—signals checked by unit tests, symbolic solvers, or strict formatting rules—to train reasoning behaviors in math and code (Wen et al., 2025). Outcome-supervised optimization methods built around GRPO and variants have shown strong empirical performance (Shao et al., 2024; Liu et al., 2025), but they often inherit a core limitation of sparse supervision: many pipelines assign near-uniform reward across a successful trajectory, blurring credit across the chain and encouraging unnecessary detours or excessive self-verification (Xie et al., 2025; Peng et al., 2025; Chen et al., 2025). Our approach addresses this bottleneck by deriving dense process rewards from a geometry-defined potential over latent states.

Potential-based reward shaping. Potential-based reward shaping (PBRS) converts a state potential into dense transition rewards while preserving optimal policies under standard conditions (Ng et al., 1999; Wiewiora, 2003; Devlin & Kudenko, 2012). Classical potentials often derive from task-specific distances in navigation or planning. We adopt the same principle, but define the potential on a root-centered hyperbolic latent space induced by backbone hidden states, so that distance-to-goal can be computed on reasoning trees.

Search-based reasoning and MCTS for LLMs. Tree-structured inference such as Tree-of-Thoughts and related planning formulations improve reasoning by exploring multiple partial solutions (Yao et al., 2023; Hao et al., 2023). Several works avoid purely heuristic search by learning value functions or reward models to guide expansion, including AlphaZero-like designs and MCTS-based self-training (Feng et al., 2023; Zhang et al., 2024; Guan et al., 2025; Xie et al., 2024).

5. Conclusion and Discussion

Empirical results suggest that negative-curvature latent geometry is a practical interface for aligning search, reward shaping, and value estimation with the branching structure of agentic reasoning.

5.1. Discussion: unifying post-training via latent preference shaping

Supervised fine-tuning (SFT) on annotated reasoning traces is token-level maximum likelihood under teacher forcing. Given a reference trajectory $\tau^* = \{(s_t^*, a_t^*)\}_{t=1}^T$ (e.g., an annotated chain-of-thought or tool-call trace), SFT minimizes

$$\mathcal{L}_{\text{SFT}}(\theta) = -\mathbb{E}_{\tau^* \sim \mathcal{D}_{\text{SFT}}} \sum_{t=1}^T \log \pi_\theta(a_t^* | s_t^*). \quad (16)$$

Here each s_t^* is constructed from ground-truth prefixes, so training is performed on the expert state distribution rather than on the model’s own rollouts. This distribution mismatch is a well-known source of compounding errors over long horizons (often referred to as exposure bias in sequence generation and covariate shift in imitation learning), where small local mistakes can quickly push the model into unseen states (Bengio et al., 2015; Ranzato et al., 2015).

LAPHA suggests a complementary view: instead of treating correctness annotations as a policy to execute, we can treat them as anchors that induce a preference signal over the model’s own sampled actions. Ignoring the clipping for exposition, the policy-gradient updates can be written as a weighted log-likelihood update on on-policy samples:

$$\nabla_\theta J(\theta) = \mathbb{E}_{\tau \sim \pi_{\theta_{\text{old}}}} \left[\hat{A}(\tau) \sum_{t=1}^T \nabla_\theta \log \pi_\theta(a_t | s_t) \right], \quad (17)$$

where $\hat{A}(\tau)$ is a centered group advantage shared across tokens of the same rollout. Thus, the update increases the probability of the model’s own actions in proportion to a preference weight $\hat{A}(\tau)$, rather than forcing exact imitation of a teacher trajectory. In LAPHA, this preference weight is derived from latent-space progress: the Poincaré potential assigns dense intermediate rewards so trajectories that move closer to verified correctness receive larger advantages.

When correctness annotations are available, they can be incorporated without executing the annotated policy. Concretely, we embed an annotated trace into the same root-centered Poincaré latent space and treat its latent

states as an additional goal-anchor set \mathcal{Y}^* . Then the goal distance can be computed against both verified-correct leaves and the annotation anchors:

$$d_i^{[\text{goal}]} = \min_{\mathbf{y} \in \mathcal{Y}^+ \cup \mathcal{Y}^*} d_{\mathbb{D}}(\mathbf{y}_i, \mathbf{y}), \quad (18)$$

while the potential and step rewards remain unchanged. This turns discrete correctness supervision into a shaped preference over the model’s on-policy rollouts, providing a path to inject annotated knowledge into RLVR even when the model rarely discovers “good cases” by itself. In the limiting case where the preference weights collapse to a binary indicator on the annotated trajectory, the objective recovers standard SFT; LAPHA corresponds to the softer, geometry-induced regime where supervision is expressed as a graded preference over the model’s current policy support.

Acknowledgment

This work was supported by a project of the Shanghai Municipal Commission of Economy and Informatization (No. 2025-GZL-RGZN-BTBX-01011).

References

- Aime problems and solutions. Art of Problem Solving Wiki. URL https://artofproblemsolving.com/wiki/index.php/AIME_Problems_and_Solutions. Accessed: 2026-01-23.
- Beardon, A. F. *The geometry of discrete groups*, volume 91. Springer Science & Business Media, 2012.
- Beeching, E., Huang, S. C., Jiang, A., Li, J., Lipkin, B., Qina, Z., Rasul, K., Shen, Z., Soletskyi, R., and Tunstall, L. Numinamath 7b tir. <https://huggingface.co/AI-M0/NuminaMath-7B-TIR>, 2024.
- Bengio, S., Vinyals, O., Jaitly, N., and Shazeer, N. Scheduled sampling for sequence prediction with recurrent neural networks. *Advances in neural information processing systems*, 28, 2015.
- Chen, X., Xu, J., Liang, T., He, Z., Pang, J., Yu, D., Song, L., Liu, Q., Zhou, M., Zhang, Z., Wang, R., Tu, Z., Mi, H., and Yu, D. Do not think that much for $2+3=?$ on the overthinking of long reasoning models. ICML 2025 Poster (abstract), 2025. Accessed via ICML 2025 virtual site.
- Devlin, S. M. and Kudenko, D. Dynamic potential-based reward shaping. In *11th International Conference on Autonomous Agents and Multiagent Systems (AAMAS 2012)*, pp. 433–440. IFAAMAS, 2012.
- Farquhar, S., Kossen, J., Kuhn, L., and Gal, Y. Detecting hallucinations in large language models using semantic entropy. *Nature*, 630(8017):625–630, 2024.
- Feng, X., Wan, Z., Wen, M., McAleer, S. M., Wen, Y., Zhang, W., and Wang, J. Alphazero-like tree-search can guide large language model decoding and training. *arXiv preprint arXiv:2309.17179*, 2023.
- Ganea, O., Bécigneul, G., and Hofmann, T. Hyperbolic neural networks. *Advances in neural information processing systems*, 31, 2018.
- Guan, X., Zhang, L. L., Liu, Y., Shang, N., Sun, Y., Zhu, Y., Yang, F., and Yang, M. rstar-math: Small llms can master math reasoning with self-evolved deep thinking. *arXiv preprint arXiv:2501.04519*, 2025.
- Hao, S., Gu, Y., Ma, H., Hong, J., Wang, Z., Wang, D., and Hu, Z. Reasoning with language model is planning with world model. In *Proceedings of the 2023 Conference on Empirical Methods in Natural Language Processing*, pp. 8154–8173, 2023.
- He, C., Luo, R., Bai, Y., Hu, S., Thai, Z., Shen, J., Hu, J., Han, X., Huang, Y., Zhang, Y., et al. Olympiad-bench: A challenging benchmark for promoting agi with olympiad-level bilingual multimodal scientific problems. In *Proceedings of the 62nd Annual Meeting of the Association for Computational Linguistics (Volume 1: Long Papers)*, pp. 3828–3850, 2024.
- Hendrycks, D., Burns, C., Kadavath, S., Arora, A., Basart, S., Tang, E., Song, D., and Steinhardt, J. Measuring mathematical problem solving with the math dataset. *arXiv preprint arXiv:2103.03874*, 2021.
- Liu, Z., Chen, C., Li, W., Qi, P., Pang, T., Du, C., Lee, W. S., and Lin, M. Understanding r1-zero-like training: A critical perspective. *arXiv preprint arXiv:2503.20783*, 2025.
- Maaten, L. v. d. and Hinton, G. Visualizing data using t-sne. *Journal of machine learning research*, 9(Nov):2579–2605, 2008.
- Ng, A. Y., Harada, D., and Russell, S. Policy invariance under reward transformations: Theory and application to reward shaping. In *Icml*, volume 99, pp. 278–287. Citeseer, 1999.
- Nickel, M. and Kiela, D. Poincaré embeddings for learning hierarchical representations. *Advances in neural information processing systems*, 30, 2017.

- Peng, K., Ding, L., Ouyang, Y., Fang, M., and Tao, D. Revisiting overthinking in long chain-of-thought from the perspective of self-doubt. *arXiv preprint arXiv:2505.23480*, 2025.
- Poincaré, H. Théorie des groupes fuchsiens. *Acta Mathematica*, 1:1–62, 1882.
- Ranzato, M., Chopra, S., Auli, M., and Zaremba, W. Sequence level training with recurrent neural networks. *arXiv preprint arXiv:1511.06732*, 2015.
- Schulman, J., Wolski, F., Dhariwal, P., Radford, A., and Klimov, O. Proximal policy optimization algorithms. *arXiv preprint arXiv:1707.06347*, 2017.
- Shao, Z., Wang, P., Zhu, Q., Xu, R., Song, J., Bi, X., Zhang, H., Zhang, M., Li, Y., Wu, Y., et al. Deepseekmath: Pushing the limits of mathematical reasoning in open language models. *arXiv preprint arXiv:2402.03300*, 2024.
- Silver, D., Schrittwieser, J., Simonyan, K., Antonoglou, I., Huang, A., Guez, A., Hubert, T., Baker, L., Lai, M., Bolton, A., et al. Mastering the game of go without human knowledge. *nature*, 550(7676):354–359, 2017.
- Wang, S., Yu, L., Gao, C., Zheng, C., Liu, S., Lu, R., Dang, K., Chen, X., Yang, J., Zhang, Z., et al. Beyond the 80/20 rule: High-entropy minority tokens drive effective reinforcement learning for llm reasoning. *arXiv preprint arXiv:2506.01939*, 2025.
- Wang, X., Wei, J., Schuurmans, D., Le, Q., Chi, E., Narang, S., Chowdhery, A., and Zhou, D. Self-consistency improves chain of thought reasoning in language models. *arXiv preprint arXiv:2203.11171*, 2022.
- Wen, X., Liu, Z., Zheng, S., Ye, S., Wu, Z., Wang, Y., Xu, Z., Liang, X., Li, J., Miao, Z., et al. Reinforcement learning with verifiable rewards implicitly incentivizes correct reasoning in base llms. *arXiv preprint arXiv:2506.14245*, 2025.
- Wiewiora, E. Potential-based shaping and q-value initialization are equivalent. *Journal of Artificial Intelligence Research*, 19:205–208, 2003.
- Xie, G., Shi, Y., Tian, H., Yao, T., and Zhang, X. Capo: Towards enhancing llm reasoning through verifiable generative credit assignment. *arXiv e-prints*, pp. arXiv–2508, 2025.
- Xie, Y., Goyal, A., Zheng, W., Kan, M.-Y., Lillicrap, T. P., Kawaguchi, K., and Shieh, M. Monte carlo tree search boosts reasoning via iterative preference learning. *arXiv preprint arXiv:2405.00451*, 2024.
- Yang, A., Li, A., Yang, B., Zhang, B., Hui, B., Zheng, B., Yu, B., Gao, C., Huang, C., Lv, C., et al. Qwen3 technical report. *arXiv preprint arXiv:2505.09388*, 2025.
- Yao, S., Zhao, J., Yu, D., Du, N., Shafran, I., Narasimhan, K. R., and Cao, Y. React: Synergizing reasoning and acting in language models. In *The eleventh international conference on learning representations*, 2022.
- Yao, S., Yu, D., Zhao, J., Shafran, I., Griffiths, T., Cao, Y., and Narasimhan, K. Tree of thoughts: Deliberate problem solving with large language models. *Advances in neural information processing systems*, 36:11809–11822, 2023.
- Yu, Q., Zhang, Z., Zhu, R., Yuan, Y., Zuo, X., Yue, Y., Dai, W., Fan, T., Liu, G., Liu, L., et al. Dapo: An open-source llm reinforcement learning system at scale. *arXiv preprint arXiv:2503.14476*, 2025.
- Zhang, B. and Sennrich, R. Root mean square layer normalization. *Advances in neural information processing systems*, 32, 2019.
- Zhang, D., Zhoubian, S., Hu, Z., Yue, Y., Dong, Y., and Tang, J. Rest-mcts*: Llm self-training via process reward guided tree search. *Advances in Neural Information Processing Systems*, 37:64735–64772, 2024.
- Zhang, X., Li, C., Zong, Y., Ying, Z., He, L., and Qiu, X. Evaluating the performance of large language models on gaokao benchmark. *arXiv preprint arXiv:2305.12474*, 2023.
- Zhang, Z., Zheng, C., Wu, Y., Zhang, B., Lin, R., Yu, B., Liu, D., Zhou, J., and Lin, J. The lessons of developing process reward models in mathematical reasoning. *arXiv preprint arXiv:2501.07301*, 2025.

A. Appendix

A.1. Monte Carlo Tree Search

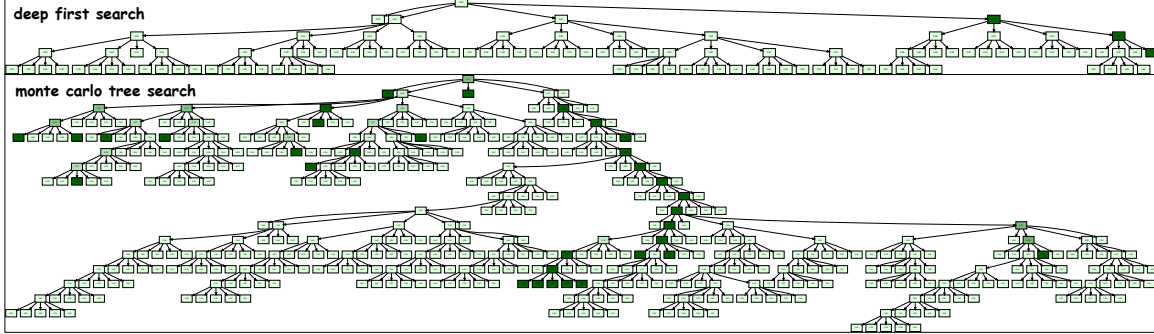


Figure 5. Rollout Trees

This appendix specifies the MCTS procedure used in LAPHA, including the search space, maintained statistics, the PUCT selection rule, likelihood-induced priors, value-based initialization, terminal-only backup, and latent-space pruning.

Search space and statistics. MCTS is performed over step-wise assistant actions. A node corresponds to a dialogue state s (messages plus any tool feedback), and an edge corresponds to choosing one candidate completion a (ending with an end-of-turn token), leading to the next state $s' = \text{apply_chat_template}(s, a)$. For each state-action edge (s, a) , we maintain a visit count $N(s, a)$ and an empirical action value $Q(s, a)$, defined as the running mean of terminal returns backed up through that edge. We write $N(s) = \sum_b N(s, b)$ for the total visits over outgoing edges. For edges that have not received any terminal backup, we keep an initialization value $Q_0(s, a)$ (defined below) which is used only for selection.

Selection (PUCT). Starting from the root s_0 , we repeatedly select actions by

$$a^*(s) = \arg \max_a \left(\hat{Q}(s, a) + c P(s, a) \frac{\sqrt{N(s)}}{1 + N(s, a)} \right), \quad (19)$$

where c is the exploration constant and $P(s, a)$ is a prior over candidate actions sampled at s . The effective value is defined as

$$\hat{Q}(s, a) = \begin{cases} Q(s, a), & N(s, a) > 0, \\ Q_0(s, a), & N(s, a) = 0. \end{cases} \quad (20)$$

Expansion and likelihood prior. When an expandable leaf state s is reached, we sample B candidate completions $\{a_k\}_{k=1}^B$ from the current policy. For a sampled completion $a_k = (a_{k,1}, \dots, a_{k,|a_k|})$, we compute its cumulative log-probability

$$p(s, a_k) = \sum_{t=1}^{|a_k|} \log \pi_\theta(a_{k,t} | s, a_{k,<t}), \quad (21)$$

and define the sibling prior by softmax normalization,

$$P(s, a_k) = \frac{\exp(p(s, a_k))}{\sum_{j=1}^B \exp(p(s, a_j))}. \quad (22)$$

Evaluation and initialization. For each newly created child $s' = \text{apply_chat_template}(s, a)$, we compute its pooled representation $\bar{\mathbf{h}}(s')$ (and cache its latent state $\mathbf{y}_{s'}$), and obtain the value prediction $f_\theta(\bar{\mathbf{h}}(s'))$. Before

any terminal backup is observed on (s, a) , we initialize its value for selection by mixing the value head with the likelihood prior,

$$Q_0(s, a) = \eta f_\theta(\bar{\mathbf{h}}(s')) + (1 - \eta) P(s, a), \quad (23)$$

where $\eta \in [0, 1]$ is a fixed mixing weight.

Backup (terminal-only). A state is marked terminal if it triggers explicit answer extraction, reaches the depth limit, degenerates into echo/repetition, or hits a context-length limit. Terminal nodes receive a verifiable return $R \in [0, 1]$ from rule-based reward functions. Only these terminal outcomes are backed up: for every traversed edge (s, a) on the selected path, we update

$$\begin{aligned} N(s, a) &\leftarrow N(s, a) + 1, \\ Q(s, a) &\leftarrow Q(s, a) + \frac{R - Q(s, a)}{N(s, a)}. \end{aligned} \quad (24)$$

Non-terminal value predictions are used only as a heuristic for selection and are not treated as ground-truth returns.

Latent-space pruning. To mitigate paraphrastic aliasing, we periodically prune the search frontier using the same root-centered Poincaré latent space. We cluster visited non-terminal nodes by hyperbolic distance and disable a fraction of nodes within each cluster, then rebuild the frontier and continue search.

Algorithm 1 LAPHA MCTS with value guidance and latent-space pruning

Require: Root prompt p_0 ; policy π_θ ; value head f_θ ; rollout budget N_{sim} ; branching factor B ; exploration constant c ; mixing weight η ; prune interval K ; prune ratio ρ
Ensure: Search tree \mathcal{T} with cached latents and edge statistics

- 1: Initialize root state $s_0 \leftarrow p_0$ and tree $\mathcal{T} \leftarrow \{s_0\}$
- 2: Initialize all edge statistics $N(s, a) \leftarrow 0$, $Q(s, a) \leftarrow 0$
- 3: **for** $n = 1, 2, \dots, N_{\text{sim}}$ **do**
- 4: $(\mathcal{P}, s) \leftarrow \text{SELECT}(\mathcal{T}, s_0, c)$
- 5: **if** s is terminal **then**
- 6: $R \leftarrow \text{REWARD}(s)$
- 7: $\text{BACKUP}(\mathcal{P}, R)$
- 8: **continue**
- 9: **end if**
- 10: Sample B candidate completions $\mathcal{A} = \{a_k\}_{k=1}^B$ from $\pi_\theta(\cdot | s)$
- 11: Compute cumulative log-probabilities $\{p(s, a_k)\}$ and priors $P(s, a_k) \leftarrow \text{softmax}(\{p(s, a_k)\})$
- 12: **for all** $a \in \mathcal{A}$ **do**
- 13: Create child $s' \leftarrow \text{apply_chat_template}(s, a)$ and add s' to \mathcal{T}
- 14: Evaluate $f_\theta(\bar{\mathbf{h}}(s'))$ and cache latent $\mathbf{y}_{s'}$ (batched in practice)
- 15: Set $Q_0(s, a) \leftarrow \eta f_\theta(\bar{\mathbf{h}}(s')) + (1 - \eta) P(s, a)$
- 16: **if** s' is terminal **then**
- 17: $R \leftarrow \text{REWARD}(s')$
- 18: $\text{BACKUP}(\mathcal{P} \cup \{(s, a)\}, R)$
- 19: **end if**
- 20: **end for**
- 21: **if** $n \bmod K = 0$ **then**
- 22: $\mathcal{T} \leftarrow \text{PRUNE}(\mathcal{T}, \rho)$
- 23: **end if**
- 24: **end for**
- 25: **return** \mathcal{T}

A.2. Should Value Supervision Update the Backbone?

We isolate whether the value regression loss should be allowed to modify the shared backbone representation that also supports generation. We compare two configurations under identical rollout, optimization, and evaluation settings: (a) **full joint training**, where gradients from the value regression loss are propagated into the backbone; and (b) a **stop-gradient** variant, where the value head is trained but its regression loss does not update the backbone (only the policy loss updates the shared layers).

Figure 6 shows a consistent long-horizon advantage for full joint training. In the early phase of training, the stop-gradient variant can preserve the initial policy behavior more closely, but it plateaus earlier: the value MSE

Algorithm 2 SELECT, BACKUP, and latent-space PRUNE

```

1: function SELECT( $\mathcal{T}, s_0, c$ )
2:    $s \leftarrow s_0$ ;  $\mathcal{P} \leftarrow []$ 
3:   while  $s$  is expanded and  $s$  is not terminal do
4:      $a^*(s) \leftarrow \arg \max_a \left( \hat{Q}(s, a) + c P(s, a) \frac{\sqrt{N(s)}}{1+N(s, a)} \right)$ 
5:     Append  $(s, a^*(s))$  to  $\mathcal{P}$ 
6:      $s \leftarrow \text{Child}(s, a^*(s))$ 
7:   end while
8:   return  $(\mathcal{P}, s)$ 
9: end function
10: function BACKUP( $\mathcal{P}, R$ )
11:   for all  $(s, a)$  in  $\mathcal{P}$  do
12:      $N(s, a) \leftarrow N(s, a) + 1$ 
13:      $Q(s, a) \leftarrow Q(s, a) + \frac{R - Q(s, a)}{N(s, a)}$ 
14:   end for
15: end function
16: function PRUNE( $\mathcal{T}, \rho$ )
17:   Let  $\mathcal{U}$  be all non-terminal, non-disabled nodes in  $\mathcal{T}$  with cached latents  $\mathbf{y}(\cdot)$ 
18:   Cluster nodes in  $\mathcal{U}$  by hyperbolic distance  $d_{\mathbb{D}}(\mathbf{y}_i, \mathbf{y}_j)$ 
19:   for all clusters  $C$  do
20:     Disable a fraction  $\rho$  of nodes in  $C$  to reduce near-duplicate branches
21:   end for
22:   Rebuild the frontier from remaining expandable nodes
23:   return  $\mathcal{T}$ 
24: end function

```

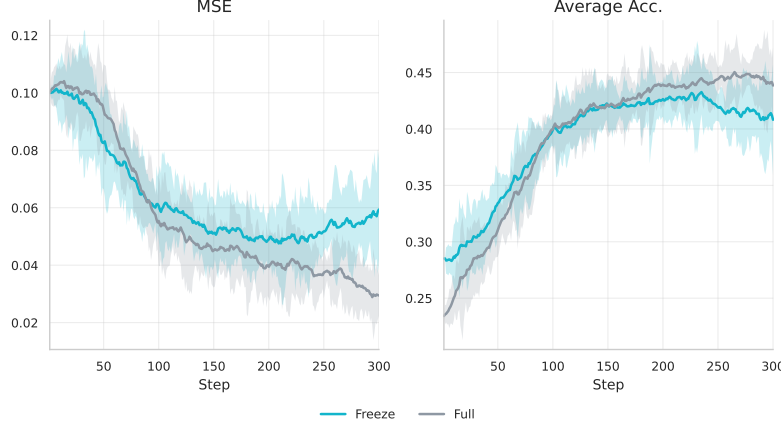


Figure 6. Ablation on whether the value regression loss is allowed to update the backbone (full vs. freeze), reported by the value MSE and the resulting average correct rate.

decreases more slowly and the average correct rate saturates at a lower level. In contrast, when the backbone is allowed to receive value gradients, the model continues to improve in both value calibration (lower MSE) and outcome quality (higher average correct rate).

This result suggests that the geometry-driven targets are not merely useful as a post-hoc critic for search-time reranking. Instead, they provide an additional learning signal that reshapes the internal representation so that progress becomes more readable from the shared pooled features $\bar{\mathbf{h}}_i$. Since the policy head and value head operate on the same latent, improving the representation for value prediction can also improve generation quality, rather than only enabling better selection at inference. Concretely, on MATH500 the fully joint model reaches **76.4%** average accuracy, compared to **67.2%** for the stop-gradient variant under identical settings.

A.3. Cold Start Hyper-parameters

```

#### model
model_name_or_path:
trust_remote_code: true

#### method
stage: sft
do_train: true
finetuning_type: full
deepspeed: ds_z3_config.json

#### dataset
dataset: numinaMath-TIR,glaive_toolcall_100k,open_r1_math_220k
template: qwen
overwrite_cache: true
preprocessing_num_workers: 16
dataLoader_num_workers: 4

#### output
output_dir:
logging_steps: 1
save_steps: 250
plot_loss: true
overwrite_output_dir: true
save_only_model: false
report_to: tensorboard

#### train
per_device_train_batch_size: 16
gradient_accumulation_steps: 8
learning_rate: 1.0e-5
num_train_epochs: 2.0
lr_scheduler_type: cosine
warmup_ratio: 0.1
bf16: true

```

A.4. Re-Formated NuminaMath-TIR

```

1 [
2   {
3     "conversations": [
4       {
5         "from": "system",
6         "value": "SOLVE THE PROBLEM STEP-BY-STEP. PRESENT THE ANSWER TO EXIT THE LOOP.\n\n\n# Guidelines\n-> Each assistant response must contain exactly one \"<think>...</think>\" block.\n- If the\nfinal answer is ready, use \"<answer>...</answer>\" block to terminate the loop.\n- No\ncontent other than whitespace may appear outside these tags.\n-> Begin every response with \"\nSTEP-(\\d+):\\n<think>...\", 1 step per response."
7     },
8     {
9       "from": "human",
10      "value": "What is the coefficient of  $x^2y^6$  in the expansion of  $\left(\frac{3}{5}x - \frac{y}{2}\right)^8$ ? Express your answer as a common fraction."
11    },
12    {
13      "from": "gpt",
14      "value": "STEP-1:\n<think>To determine the coefficient of  $x^2y^6$  in the expansion of  $\left(\frac{3}{5}x - \frac{y}{2}\right)^8$ , we can use the binomial theorem.\n\nThe binomial theorem states:  $\sum_{k=0}^n \binom{n}{k} a^{n-k} b^k$ . In this case,  $a = \frac{3}{5}x$ ,  $b = -\frac{y}{2}$ , and  $n = 8$ . We are interested in the term that contains  $x^2y^6$ . In the general term of the binomial expansion:  $\binom{8}{k} \left(\frac{3}{5}x\right)^{8-k} \left(-\frac{y}{2}\right)^k$ , we need  $8 - k = 2$ , thus  $k = 6$ . Substituting  $k = 6$  into the expression:  $\binom{8}{6} \left(\frac{3}{5}x\right)^2 \left(-\frac{y}{2}\right)^6 = \binom{8}{6} \left(\frac{3}{5}x\right)^2 \left(-\frac{y}{2}\right)^6$ . Now, we will compute each part of this expression.\n\n1. Calculate the binomial coefficient  $\binom{8}{6}$ . Compute  $\left(\frac{3}{5}\right)^2$ . Compute  $\binom{8}{6}$ . Compute  $\left(-\frac{y}{2}\right)^6$ . Compute  $\left(\frac{3}{5}x\right)^2$ . Compute  $\left(-\frac{y}{2}\right)^6$ . Combine everything together to get the coefficient of  $x^2y^6$ . Let's compute these in Python.\n</think>\n<tool_call>\n  "name": "execute_python_code",\n  "arguments": {\n    "code": "from math import comb\n\nGiven\nvalues\nn = 8\nk = 6\n\n# Calculate the binomial coefficient\nbinom_coeff = comb(n, k)\n\n# Compute (3/5)^2\na_term = (3/5)**2\n\n# Compute (-1/2)^6\nb_term = (-1/2)**6\n\n# Combine terms to get the coefficient of x^2y^6\ncoefficient = binom_coeff * a_term * b_term\n\nprint(coefficient)\n\n</tool_call>\n"
15   }

```

```

16
17     "from": "human",
18     "value": "<tool_response>\nVar: comb; Type: builtin_function_or_method\n<built-in function comb>\n    nVar: n; Type: int\n8\nVar: k; Type: int\n6\nVar: binom_coeff; Type: int\n28\nVar: a_term;\n    Type: float\n0.36\nVar: b_term; Type: float\n0.015625\nVar: coefficient; Type: float\n0.1575\n</tool_response>"
19
20 },
21 {
22     "from": "gpt",
23     "value": "STEP-2:\n<think>The coefficient of  $(x^2y^6)$  in the expansion of  $\left(\frac{3}{5}x - \frac{1}{400}\right)^8$  is  $0.1575$ . To express this as a common fraction, we recognize that  $0.1575 = \frac{1575}{10000} = \frac{63}{400}$ . Thus, the coefficient can be expressed as  $\frac{63}{400}$ .</think>\n<answer>\frac{63}{400}</answer>"
24
25 },
26 "tools": "[{"type": "function", "function": {"name": "execute_python_code", "description": "\nExecute Python code in a sandboxed environment.\nUsage (two equivalent forms):\n1) As a tool_call block with JSON arguments, e.g.:\n    {\n        \"name\": \"execute_python_code\"\n    }\n2) As a fenced code block after <think></think>:\n    <think>\n        python\n        ... code ...\n    </think>\n\nThe system automatically converts the fenced block into a tool call.\nReturn behavior:\n- Only variables that were explicitly assigned in the code (latest 10) are displayed.\n- Module objects are ignored.\n- print() output is captured and included.\nDisplay policy:\n- Long strings and large arrays are truncated.\n- DataFrame and Series outputs include only head/tail samples.\n- Default timeout: 10 seconds.\n\nparameters": {"type": "object", "properties": {"code": {"type": "string"}, "description": "Python source code to execute. Assign the variables you want to show, for example:\n    result = solve(...)\n    summary = df.describe()\n"}, "required": ["code"]}}]"
27 ]
```

A.5. RL Hyper-parameters

```

# Model arguments
model_name_or_path:
output_dir:
model_revision: main
torch_dtype: bfloat16
attn_IMPLEMENTATION: flash_attention_2
bf16: true
tf32: true

# Training arguments
num_train_epochs: 8
per_device_train_batch_size: 16
gradient_accumulation_steps: 1
gradient_checkpointing: true
gradient_checkpointing_kwargs:
    use_reentrant: false
learning_rate: 1.0e-6
lr_scheduler_type: cosine
warmup_ratio: 0.05

# MCTS
depth: 6
breadth: 6
num_sim: 24
prune_per: 8
passk_threshold: 1.0
enable_thinking: false

beta: 1.0e-8
loss_type: dr_grop
value_head_type: linear

# vLLM
use_vllm: true
vllm_mode: server
vllm_server_host: 0.0.0.0
vllm_server_port: 8000
vllm_server_timeout: 60

max_prompt_length: 3072
max_completion_length: 1024
temperature: 0.7
```

```
repetition_penalty: 1.05
top_p: 0.8
top_k: 20
```

A.6. Math Examples

PROMPT

```
# User Question:
Solve the following math problem step by step. You have two action that you
can do thinking and answering. Plz put your thinking in a <think></think>
block, and answer in a <answer></answer> block. Question:
Let $$ be the solid in three-dimensional space consisting of all points (
$x, y, z$ ) satisfying the following system of six simultaneous conditions:
$$
\begin{aligned}
& x \geq 0, \quad y \geq 0, \quad z \geq 0 \\
& x+y+z \leq 11, \\
& 2x+4y+3z \leq 36 \\
& 2x+3z \leq 24.
\end{aligned}
\end{aligned}
$$

Determine the number $v$ of vertices of $S$.

<im_start>assistant
STEP-1:
<think>
To determine the number of vertices of the solid $(S)$, we need to find
the points where the boundaries of the inequalities intersect. Each vertex
of the solid is a point where three inequalities meet. We need to solve the
system of equations formed by the intersections of these inequalities.

The inequalities are:
1. $(x \geq 0)$
2. $(y \geq 0)$
3. $(z \geq 0)$
4. $(x + y + z \leq 11)$
5. $(2x + 4y + 3z \leq 36)$
6. $(2x + 3z \leq 24)$

To find the vertices, we will solve the system of equations formed by
setting the inequalities as equalities and checking for non-negative
solutions.
</think><im_end>
<im_start>assistant
STEP-2:
<think>
We will solve the following systems of equations to find the vertices:
1. $(x + y + z = 11), (2x + 4y + 3z = 36), (2x + 3z = 24)$
2. $(x + y + z = 11), (2x + 4y + 3z = 36), (z = 0)$
3. $(x + y + z = 11), (2x + 4y + 3z = 36), (y = 0)$
4. $(x + y + z = 11), (2x + 3z = 24), (z = 0)$
5. $(x + y + z = 11), (2x + 3z = 24), (y = 0)$
6. $(2x + 4y + 3z = 36), (2x + 3z = 24), (z = 0)$
7. $(2x + 4y + 3z = 36), (2x + 3z = 24), (y = 0)$
8. $(2x + 4y + 3z = 36), (z = 0), (y = 0)$
9. $(2x + 3z = 24), (y = 0), (z = 0)$
10. $(x + y + z = 11), (z = 0), (y = 0)$
11. $(x + y + z = 11), (2x + 4y = 36), (z = 0)$

Let's solve these systems step by step.
</think>
```

```

<tool_call>
{"name": "execute_python_code", "arguments": {"code": "from sympy import
symbols, Eq, solve\n\nx, y, z = symbols('x y z')\n\n# System 1\nneq1 = Eq(x +
y + z, 11)\nneq2 = Eq(2*x + 4*y + 3*z, 36)\nneq3 = Eq(2*x + 3*z, 24)\n\n# Solve the
system\nnsolution1 = solve((eq1, eq2, eq3), (x, y, z))\n\n# System 2\nneq4 = Eq(2*x + 4*y + 3*z, 36)\nneq5 = Eq(z, 0)\n\n# Solve the
system\nnsolution2 = solve((eq1, eq4, eq5), (x, y, z))\n\n# System 3\nneq6 =
Eq(2*x + 4*y + 3*z, 36)\nneq7 = Eq(y, 0)\n\n# Solve the system\nnsolution3 =
solve((eq1, eq6, eq7), (x, y, z))\n\n# System 4\nneq8 = Eq(x + y + z,
11)\nneq9 = Eq(2*x + 3*z, 24)\nneq10 = Eq(z, 0)\n\n# Solve the
system\nnsolution4 = solve((eq8, eq9, eq10), (x, y, z))\n\n# System 5\nneq11 =
Eq(x + y + z, 11)\nneq12 = Eq(2*x + 3*z, 24)\nneq13 = Eq(y, 0)\n\n# Solve the
system\nnsolution5 = solve((eq11, eq12, eq13), (x, y, z))\n\n# System 6\nneq14 =
Eq(2*x + 4*y + 3*z, 36)\nneq15 = Eq(2*x + 3*z, 24)\nneq16 = Eq(z, 0)\n\n# Solve the
system\nnsolution6 = solve((eq14, eq15, eq16), (x, y, z))\n\n# System 7\nneq17 =
Eq(2*x + 4*y + 3*z, 36)\nneq18 = Eq(2*x + 3*z, 24)\nneq19 =
Eq(y, 0)\n\n# Solve the system\nnsolution7 = solve((eq17, eq18, eq19), (x, y,
z))\n\n# System 8\nneq20 = Eq(2*x + 4*y + 3*z, 36)\nneq21 = Eq(z, 0)\nneq22 =
Eq(y, 0)\n\n# Solve the system\nnsolution8 = solve((eq20, eq21, eq22), (x, y,
z))\n\n# System 9\nneq23 = Eq(2*x + 3*z, 24)\nneq24 = Eq(y, 0)\nneq25 = Eq(z,
0)\n\n# Solve the system\nnsolution9 = solve((eq23, eq24, eq25), (x, y,
z))\n\n# System 10\nneq26 = Eq(x + y + z, 11)\nneq27 = Eq(z, 0)\nneq28 = Eq(y,
0)\n\n# Solve the system\nnsolution10 = solve((eq26, eq27, eq28), (x, y,
z))\n\n# System 11\nneq29 = Eq(x + y + z, 11)\nneq30 = Eq(2*x + 4*y, 36)\nneq31 =
Eq(z, 0)\n\n# Solve the system\nnsolution11 = solve((eq29, eq30, eq31), (x,
y, z))\n\nnsolution1, solution2, solution3, solution4, solution5, solution6,
solution7, solution8, solution9, solution10, solution11"}}
</tool_call><|im_end|>
<|im_start|>user
<tool_response>
Var: eq25; Type: Equality
Eq(z, 0)
Var: solution9; Type: dict
dict(dict_items([(x, 12), (y, 0), (z, 0)]))
Var: eq26; Type: Equality
Eq(x + y + z, 11)
Var: eq27; Type: Equality
Eq(z, 0)
Var: eq28; Type: Equality
Eq(y, 0)
Var: solution10; Type: dict
dict(dict_items([(x, 11), (y, 0), (z, 0)]))
Var: eq29; Type: Equality
Eq(x + y + z, 11)
Var: eq30; Type: Equality
Eq(2*x + 4*y, 36)
Var: eq31; Type: Equality
Eq(z, 0)
Var: solution11; Type: dict
dict(dict_items([(x, 4), (y, 7), (z, 0)]))
</tool_response><|im_end|>
<|im_start|>assistant

```

COMPLETION

STEP-3:
<think>
We have solved the systems of equations and found the following solutions:
1. $\{(x, y, z) = (3, 5, 3)\}$

```

2. \((x, y, z) = (9, 2, 0)\)
3. \((x, y, z) = (7, 0, 4)\)
4. \((x, y, z) = (11, 0, 0)\)
5. \((x, y, z) = (6, 0, 0)\)
6. \((x, y, z) = (9, 0, 0)\) (This solution is a repetition of solution 2)
7. \((x, y, z) = (12, 0, 0)\) (This solution is not valid because \((x + y + z > 11)\))
8. \((x, y, z) = (0, 0, 0)\)
9. \((x, y, z) = (12, 0, 0)\) (Again, this solution is not valid)
10. \((x, y, z) = (11, 0, 0)\) (This solution is a repetition of solution 4)
11. \((x, y, z) = (4, 7, 0)\)

```

After removing the repeated and invalid solutions, we have the following unique vertices:

```

1. \((3, 5, 3)\)
2. \((9, 2, 0)\)
3. \((7, 0, 4)\)
4. \((11, 0, 0)\)
5. \((6, 0, 0)\)
6. \((0, 0, 0)\)
7. \((4, 7, 0)\)

```

Therefore, the number of vertices of the solid \mathcal{S} is 7.

</think>
<answer>7</answer>

— GROUND TRUTH —

7

— PROMPT —

<|im_start|>system
SOLVE THE PROBLEM STEP-BY-STEP. PRESENT THE ANSWER TO EXIT THE LOOP.

```

# Guidelines
→ Each assistant response must contain exactly one "<think>...</think>" block.
  · If the final answer is ready, use "<answer>...</answer>" block to terminate the loop.
  · No content other than whitespace may appear outside these tags.
→ Begin every response with "STEP-(\d+):\n<think>...", 1 step per response.<|im_end|>
<|im_start|>user

# Please answer:
Let  $\mathbf{a}$ ,  $\mathbf{b}$  and  $\mathbf{c}$  be three vectors such that  $\|\mathbf{a}\| = \|\mathbf{b}\| = \|\mathbf{c}\| = 2$ . Also, the angle between any two of these vectors is  $\arccos \frac{5}{8}$ . Find the volume of the parallelepiped generated by  $\mathbf{a}$ ,  $\mathbf{b}$  and  $\mathbf{c}$ . The answer is in the form  $\frac{m}{n}$ , where  $\gcd(m, n) = 1$ . Please provide the value of  $m + n$ .
```

```

format the FINAL answer as <answer>...</answer>.
<|im_end|>
<|im_start|>assistant
STEP-1:
<think>First, recall the formula for the volume of a parallelepiped generated by vectors  $(\mathbf{a}, \mathbf{b}, \mathbf{c})$ , which is given
```

by the absolute value of the scalar triple product $(\mathbf{a} \cdot (\mathbf{b} \times \mathbf{c}))$. This can also be expressed as the determinant of the matrix formed by the vectors as its columns (or rows).

The scalar triple product can also be calculated using the formula involving the magnitudes of the vectors and the cosine of the angles between them. Specifically, for vectors $(\mathbf{a}, \mathbf{b}, \mathbf{c})$, the volume (V) is given by:

$$[V = \|\mathbf{a}\| \|\mathbf{b}\| \|\mathbf{c}\| \sqrt{1 - \cos^2 \theta - \cos^2 \phi - \cos^2 \psi + 2 \cos \theta \cos \phi \cos \psi}]$$
 where (θ, ϕ, ψ) are the angles between the vectors. In this case, $\theta = \phi = \psi = \arccos \frac{5}{8}$.

Let's calculate the volume step by step:</think><|im_end|>
<|im_start|>user
 Please continue.<|im_end|>
<|im_start|>assistant
 STEP-2:
<think>

— COMPLETION —

STEP-2:
<think>Given $\|\mathbf{a}\| = \|\mathbf{b}\| = \|\mathbf{c}\| = 2$ and the angle between any two vectors is $\arccos \frac{5}{8}$, we substitute these values into the volume formula:

$$[V = 2 \cdot 2 \cdot 2 \cdot \sqrt{1 - \left(\frac{5}{8}\right)^2 - \left(\frac{5}{8}\right)^2 - \left(\frac{5}{8}\right)^2 + 2 \left(\frac{5}{8}\right) \left(\frac{5}{8}\right) \left(\frac{5}{8}\right)}]$$

First, we compute $(\left(\frac{5}{8}\right)^2)^2$:

$$[\left(\frac{5}{8}\right)^2 = \frac{25}{64}]$$

Then substitute and simplify inside the square root:

$$[V = 8 \cdot \sqrt{1 - 3 \cdot \frac{25}{64} + 2 \cdot \frac{125}{512}}]$$

$$[V = 8 \cdot \sqrt{1 - \frac{75}{64} + \frac{250}{512}}]$$

Convert 1 to a fraction with a denominator of 512:

$$[1 = \frac{512}{512}]$$

$$[V = 8 \cdot \sqrt{\frac{512}{512} - \frac{75}{64} \cdot \frac{512}{512} + \frac{250}{512}}]$$

$$[V = 8 \cdot \sqrt{\frac{512 - 600 + 250}{512}}]$$

$$[V = 8 \cdot \sqrt{\frac{162}{512}}]$$

Simplify the fraction inside the square root:

$$[\frac{162}{512} = \frac{81}{256}]$$

$$[V = 8 \cdot \sqrt{\frac{81}{256}}]$$

$$[V = 8 \cdot \sqrt{\frac{9}{16}}]$$

$$[V = \frac{72}{16}]$$

```
[ V = \frac{9}{2} \]
```

The volume is $\frac{9}{2}$, which is in the form $\frac{m}{n}$ with $m = 9$ and $n = 2$. Thus, $m + n = 9 + 2$.</think>

<answer>11</answer>

GROUND TRUTH

11

PROMPT

```
<|im_start|>system
SOLVE THE PROBLEM STEP-BY-STEP. PRESENT THE ANSWER TO EXIT THE LOOP.

# Guidelines
→ Each assistant response must contain exactly one "<think>...</think>" block.
  • If the final answer is ready, use "<answer>...</answer>" block to terminate the loop.
  • No content other than whitespace may appear outside these tags.
→ Begin every response with "STEP-(\d+):\n<think>...", 1 step per response.

# Tools

You may call one or more functions to assist with the user query.
```

You are provided with function signatures within `<tools></tools>` XML tags:

```
<tools>
{"type": "function", "function": {"name": "execute_python_code", "description": "Execute Python code in a sandboxed environment.\n", "parameters": {"type": "object", "properties": {"code": {"type": "string", "description": ""}}, "required": ["code"]}}}
</tools>
```

For each function call, return a json object with function name and arguments within `<tool_call></tool_call>` XML tags:

```
<tool_call>
{"name": <function-name>, "arguments": <args-json-object>}
</tool_call><|im_end|>
<|im_start|>user
```

Please answer:

The solution to the inequality

$\frac{x+c}{x^2+ax+b} \leq 0$ is $x \in (-\infty, -1) \cup [1, 2]$. Find $a+b+c$.

format the FINAL answer as <answer>...</answer>.

```
<|im_end|>
<|im_start|>assistant
```

STEP-1:

<think>

Given the inequality:

```
[ 
\frac{x+c}{x^2+ax+b} \leq 0
\]
```

we know the solution set for (x) is:

```
[  
x \in (-\infty, -1) \cup [1, 2)  
]
```

This implies that the quadratic equation in the denominator, $x^2 + ax + b$, has roots at $x = -1$ and $x = 2$, because the expression changes sign at these points. Additionally, the numerator $x + c$ must change sign at $x = 1$.

Let's start by finding the quadratic $x^2 + ax + b$ using its roots. Since the roots of the quadratic are -1 and 2 , we can write it as:

```
[  
x^2 + ax + b = (x + 1)(x - 2)  
]
```

Expanding this, we get:

```
[  
x^2 + ax + b = x^2 - x - 2  
]
```

Thus, $a = -1$ and $b = -2$.

Next, we need to determine c . The inequality $\frac{x+c}{x^2+ax+b} \leq 0$ should be satisfied for the given ranges of x . We know that $x + c$ must have a root at $x = 1$ because the inequality changes sign at this point. Therefore:

```
[  
1 + c = 0 \implies c = -1  
]
```

Now, we need to verify that the inequality holds for the given ranges:

```
[  
\frac{x - 1}{x^2 - x - 2} \leq 0  
]
```

We need to check the intervals $(-\infty, -1)$, $(-1, 1)$, $(1, 2)$, and $(2, \infty)$.

Let's analyze the sign of the expression in each interval:

1. For $x \in (-\infty, -1)$:
 - $x - 1 < 0$
 - $x^2 - x - 2 > 0$
 - Hence, $\frac{x - 1}{x^2 - x - 2} < 0$
2. For $x \in (-1, 1)$:
 - $x - 1 < 0$
 - $x^2 - x - 2 < 0$
 - Hence, $\frac{x - 1}{x^2 - x - 2} > 0$
3. For $x \in (1, 2)$:
 - $x - 1 > 0$
 - $x^2 - x - 2 < 0$
 - Hence, $\frac{x - 1}{x^2 - x - 2} < 0$
4. For $x \in (2, \infty)$:
 - $x - 1 > 0$
 - $x^2 - x - 2 > 0$
 - Hence, $\frac{x - 1}{x^2 - x - 2} > 0$

```

- \(( x - 1 > 0 \)
- \(( x^2 - x - 2 > 0 \)
- Hence, \(( \frac{x - 1}{x^2 - x - 2} > 0 \)


```

Thus, the inequality holds for $(x \in (-\infty, -1) \cup [1, 2])$.

Finally, we need to find $(a + b + c)$:

```

[
a + b + c = -1 + (-2) + (-1) = -4
\]


```

Let's confirm this result using Python code.</think>

```

<tool_call>
{"name": "execute_python_code", "arguments": {"code": "# Define the
coefficients\na = -1\nb = -2\nc = -1\n\n# Calculate a + b + c\nresult = a +
b + c\nprint(result)"}}
</tool_call><|im_end|>
<|im_start|>user
<tool_response>
----- terminal output -----
-4
-----
```

```

</tool_response><|im_end|>
<|im_start|>assistant
STEP-2:
<think>
```

— COMPLETION —

```

STEP-2:
<think>
The value of  $(a + b + c)$  is  $(\boxed{-4})$ .</think>
<answer>-4</answer>
```

— GROUND TRUTH —

```

-4
```

— PROMPT —

```

<|im_start|>system
SOLVE THE PROBLEM STEP-BY-STEP. PRESENT THE ANSWER TO EXIT THE LOOP.
```

```

# Guidelines
→ Each assistant response must contain exactly one "<think>...</think>" block.
  · If the final answer is ready, use "<answer>...</answer>" block to
  terminate the loop.
  · No content other than whitespace may appear outside these tags.
→ Begin every response with "STEP-(\d+):\n<think>...", 1 step per response.
```

```

# Tools
```

You may call one or more functions to assist with the user query.

You are provided with function signatures within <tools></tools> XML tags:

```

<tools>
{"type": "function", "function": {"name": "execute_python_code",
"description": "Execute Python code in a sandboxed environment.\n",
```

```
"parameters": {"type": "object", "properties": {"code": {"type": "string", "description": ""}}, "required": ["code"]}}
```

```
</tools>
```

For each function call, return a json object with function name and arguments within <tool_call></tool_call> XML tags:

```
<tool_call>
{"name": <function-name>, "arguments": <args-json-object>}
</tool_call><|im_end|>
<|im_start|>user
```

Please answer:

The figure below has only two sizes for its internal angles. The larger angles are three times the size of the smaller angles. Find the degree measure of one of the larger angles.

Note: The figure is a nonagon (9-sided polygon).

format the FINAL answer as <answer>...</answer>.

<|im_end|>

<|im_start|>assistant

STEP-1:

think

Given that the figure is a nonagon (9-sided polygon), we know the sum of its interior angles can be calculated using the formula for the sum of the interior angles of an (n) -sided polygon:

[\text{Sum of interior angles} = (n - 2) \times 180^\circ]

For a nonagon ($n = 9$):

$$[\text{Sum of interior angles}] = (9 - 2) \times 180^\circ = 7 \times 180^\circ = 1260^\circ$$

Let's denote the smaller angle as x degrees. Since the larger angle is three times the size of the smaller angle, it will be $3x$ degrees.

Since there are 9 angles in total, let's denote the number of smaller angles as s and the number of larger angles as l . We have:

$$\lceil s + 1 = 9 \rfloor$$

The sum of all the angles is given by:

「 sx + 31(3x) = 1260^\circ \right]

Simplifying, we get:

$$[sx + 91(3x) = 1260^\circ \text{ circ } \backslash]$$

We need to solve these equations simultaneously to find x and subsequently $3x$. Let's do this using Python.

<tool_call>

```
{"name": "execute_python_code", "arguments": {"code": "from sympy import\nsymbols, Eq, solve\n\n# Define the variables\nx, s, l = symbols('x s\nl')\n\n# Number of sides of the polygon\nn = 9\n\n# Sum of\ninterior angles of a nonagon\nnsum_of_angles = 1260\n\n# Equation for\nthe sum of angles\nneq1 = Eq(s + 1, n)\n\n# Equation for the sum of the\nangles\nneq2 = Eq(s * x + 1 * 3 * x, sum_of_angles)\n\n# Solve the\nsolution = solve((neq1, neq2), (s, x)\n\nprint(solution)"}},
```

```

system of equations\r\nsolution = solve((eq1, eq2), (s, l,
x))\r\nprint(solution)"}}
</tool_call><|im_end|>
<|im_start|>user
<tool_response>
----- terminal output -----
[(9*(3*x - 140)/(2*x), -9*(x - 140)/(2*x), x)]


-----


</tool_response><|im_end|>
<|im_start|>assistant
STEP-2:
<think>
It appears that the solution provided is in terms of  $\langle x \rangle$ , which means we need to further simplify or substitute values to find the specific value of  $\langle x \rangle$ .


Given the relationship  $\langle s + l = 9 \rangle$  and the fact that  $\langle s \rangle$  and  $\langle l \rangle$  are integers, we can iterate over possible values of  $\langle x \rangle$  to find a consistent solution.



Let's try solving for specific integer values of  $\langle x \rangle$  and check if they satisfy both equations.</think>


<tool_call>
{"name": "execute_python_code", "arguments": {"code": "# Function to check if a given x satisfies both equations\ndef check_solution(x_val):\r\n    s_val = 9 * (3 * x_val - 140) / (2 * x_val)\r\n    l_val = -9 * (x_val - 140) / (2 * x_val)\r\n    return s_val.is_integer() and l_val.is_integer(),\r\n    s_val, l_val\r\n\r\n# Iterate over possible integer values of x from 1 to 140\r\nfor x_val in range(1, 141):\r\n    is_valid, s_val, l_val =\r\n        check_solution(x_val)\r\n    if is_valid:\r\n        break\r\n\r\nprint(((x_val, s_val, l_val)))"}}

</tool_call><|im_end|>
<|im_start|>user
<tool_response>
----- terminal output -----
(4, -144.0, 153.0)


-----


</tool_response><|im_end|>
<|im_start|>assistant
STEP-3:
<think>
It seems we encountered a negative value for  $\langle s \rangle$ , which is not valid since the number of angles cannot be negative. Let's adjust our approach slightly by iterating over possible integer values of  $\langle x \rangle$  and checking the conditions more carefully.


We'll ensure  $\langle s \rangle$  and  $\langle l \rangle$  are positive integers and re-evaluate the constraints.</think>


<tool_call>
{"name": "execute_python_code", "arguments": {"code": "# Function to check if a given x satisfies both equations\ndef check_solution(x_val):\r\n    s_val = 9 * (3 * x_val - 140) / (2 * x_val)\r\n    l_val = -9 * (x_val - 140) / (2 * x_val)\r\n    return s_val.is_integer() and l_val.is_integer(),\r\n    s_val, l_val\r\n\r\n# Iterate over possible integer values of x from 1 to 140\r\nfor x_val in range(1, 141):\r\n    is_valid, s_val, l_val =\r\n        check_solution(x_val)\r\n    if is_valid:\r\n        break\r\n\r\nprint(((x_val, s_val, l_val)))"}}


```

```

</tool_call><|im_end|>
<|im_start|>user
<tool_response>
----- terminal output -----
(4, -144.0, 153.0)

-----
</tool_response><|im_end|>
<|im_start|>assistant
STEP-4:
<think>
It appears that we still encountered invalid values. Let's refine our
approach. We should consider the possibility that  $\lfloor x \rfloor$  might be a divisor
of 140, as this could help us find valid integer solutions.

We'll iterate over potential divisors of 140 and check if they satisfy the
conditions.</think>
<tool_call>
{"name": "execute_python_code", "arguments": {"code": "# List of divisors of
140\ndivisors = [1, 2, 4, 5, 7, 10, 14, 20, 28, 35, 70, 140]\n\n# Function to check if a given x satisfies both equations\n\ncheck_solution(x_val):\n    s_val = 9 * (3 * x_val - 140) / (2 *
x_val)\n    l_val = -9 * (x_val - 140) / (2 * x_val)\n    return\n    s_val.is_integer() and l_val.is_integer(), s_val, l_val\n\n# Iterate
over possible divisors of 140\nfor x_val in divisors:\n    is_valid,
    s_val, l_val = check_solution(x_val)\n    if is_valid:\n        break\n    print((x_val, s_val, l_val))"}
</tool_call><|im_end|>
<|im_start|>user
<tool_response>
----- terminal output -----
(4, -144.0, 153.0)

-----
</tool_response><|im_end|>
<|im_start|>assistant
STEP-5:
<think>
It seems that even after considering divisors of 140, we still encounter
invalid values for  $\lfloor s \rfloor$  and  $\lfloor l \rfloor$ . This suggests that our initial
assumptions might be incorrect. Let's reconsider the problem.

Given that the sum of the interior angles of a nonagon is 1260 degrees, and
knowing that the larger angles are three times the size of the smaller
angles, we can set up the following relationships:


$$[ s \cdot x + l \cdot 3x = 1260 ]$$


Since  $\lfloor s + l = 9 \rfloor$ :


$$[ s = 9 - l ]$$


Substituting  $\lfloor s \rfloor$  into the first equation:


$$[ (9 - l) \cdot x + l \cdot 3x = 1260 ]$$


This simplifies to:


$$[ 9x - lx + 3lx = 1260 ]$$


```

```

[ 9x + 21x = 1260 \]
[ x(9 + 21) = 1260 \]
[ x = \frac{1260}{9 + 21} \]

To find integer solutions for \(\( x \)\), \(\( 9 + 21 \)\) must be a divisor of 1260. Let's list the divisors of 1260 and solve for \(\( x \)\) and \(\( l \)\).

</think>
<tool_call>
{"name": "execute_python_code", "arguments": {"code": "# List of divisors of 1260\ndivisors = [1, 2, 3, 4, 5, 6, 7, 9, 10, 12, 14, 15, 18, 20, 21, 28, 30, 35, 36, 42, 45, 60, 63, 70, 84, 90, 105, 126, 140, 180, 210, 252, 315, 420, 630, 1260]\n\n# Function to check if a given x satisfies both equations\n\ndef check_solution(x_val, l_val):\n    s_val = 9 - l_val\n    if s_val > 0 and l_val > 0:\n        return True\n    return False\n\n# Iterate over possible values of l to find valid x\nfor l_val in range(1, 10):  # Reasonable range for l\n    if (9 + 2 * l_val) in divisors:\n        x_val = 1260 // (9 + 2 * l_val)\n        if check_solution(x_val, l_val):\n            break\nprint(((x_val, 3 * x_val, l_val, 9 - l_val)))"
</tool_call><|im_end|>
<|im_start|>user
<tool_response>
----- terminal output -----
(84, 252, 3, 6)

-----
</tool_response><|im_end|>
<|im_start|>assistant
STEP-6:
<think>

```

— COMPLETION —

STEP-6:
<think>
After checking the divisors of 1260, we find that when $(l = 3)$:

- The smaller angle (x) is 84 degrees.
- The larger angle $(3x)$ is 252 degrees.
- The number of smaller angles (s) is 6.
- The number of larger angles (l) is 3.

Thus, the degree measure of one of the larger angles is

\(\boxed{252}\).</think>

<answer>252</answer>

— GROUND TRUTH —

252

. Correspondence to: Siyu Zhu <siyuzhu@fudan.edu.cn>.